

Active-Transient Liquid Phase (A-TLP) Bonding of Pure Aluminum Matrix Composite Reinforced with Short Alumina Fiber Using Al-12Si-xTi Foils as Active Interlayer



GUIFENG ZHANG, WEI SU, and AKIO SUZUMURA

To optimize both the interlayer composition design route and pressure for joining aluminum matrix composite reinforced with short alumina fiber (as-cast 30 vol pct $\text{Al}_2\text{O}_{3\text{sf}}/\text{Al}$), traditional transient liquid phase (TLP) bonding using Al-12Si and Cu interlayer and active-TLP (A-TLP) bonding using an active Ti-containing interlayer (Al-12Si-xTi, $x = 0.1, 0.5,$ and 1 wt pct) under the same condition [883 K (610 °C) \times 30 minutes \times 1 or 0.015 MPa in flowing argon] were compared in terms of interfacial wettability, bond seam microstructure, shear strength, and fracture path. It was found that not only the Ti content but also the pressure are critical factors affecting interfacial wettability and bond seam microstructure. The improvement in wettability by adding Ti as an active element were confirmed by reduction of expulsion of liquid interlayer, elimination of interfacial gap, higher shear strength and favorable fracture path (partially through bond seam and the composite). Because of the incubation period for wetting, reducing the pressure after melting of the interlayer could further increase joint shear strength by thickening the remaining bond seam of solid-solution matrix and decreasing fraction of the *in situ* newly formed Al-Si-Ti IMC phase (short bar shape) within the bond seam. The maximum shear strength of 88.6 MPa (99 pct of the as-cast composite) was obtained by adding trace Ti content (0.5 Ti wt pct) addition and using low pressure (0.015 MPa). The results showed that suitable combination of Ti content and pressure pattern is required for improving both wettability and bond seam microstructure.

DOI: 10.1007/s11663-015-0371-5

© The Author(s) 2016. This article is published with open access at Springerlink.com

I. INTRODUCTION

ALTHOUGH the addition of discontinuous ceramic reinforcement into an aluminum matrix can improve the stiffness, wear resistance, and compressive strength at an elevated temperature of monolithic aluminum matrix, the presence of ceramic reinforcement in aluminum matrix composites (Al-MMCs) deteriorates the weldability primarily because of the intense and detrimental interfacial reaction between ceramic particles and superheated Al melt in arc welding.^[1-4] Thus, friction-stir welding and brazing are promising methods for joining discontinuously reinforced Al-MMCs.^[5-7] Because both Al matrix and ceramic particles coexist on the surface of Al-MMCs to be joined,^[8] the brazability of Al-MMCs is determined by the wettability at two kinds of microinterfaces: matrix/brazing filler metal (M/M) and reinforcement/brazing filler metal (R/M).^[7]

The first factor governing the wettability at both M/M and R/M interfaces is the composition design of the brazing filler metal. The published brazing filler metals can be classified into three groups with different melting regions: (I) Zn-Al(-Cu),^[9-12] (II) Al-12Si (4047),^[13,14] and Al-11.6Si-1.5Mg [4N04 with a melting range of 840 K to 850 K (567 °C to 577 °C)] systems,^[7,8,14-17] and (III) Al-28Cu-5Si-2Mg with a melting range of 798 K to 808 K (525 °C to 535 °C)^[18,19] and Al-24Cu-5Si-0.5Ni.^[20] For Zn-based filler metals, flux (hygroscopic chlorides),^[9] ultrasonic vibration,^[10,11] or stirring^[12] must be introduced to remove oxide film on the Al matrix surface at a lower joining temperature in air. For Al-Si brazing filler metal, an interfacial gap (1 μm) at R/M interface was observed,^[13] and it was easy to discharge from the joint interface under pressure, leading to the lack of dissolution of Al matrix. For Al-Si-Mg brazing filler metal, Suzumura *et al.* first demonstrated that Al-12Si-1.5Mg filler metal could spread on the surface of Al matrix composite reinforced by a short alumina fiber while Al-12Si remained in the original shape of wire in the wettability test in a vacuum.^[14] Moreover, although Al-12Si-1.5Mg brazing filler metal was able to wet Al matrix with rougher surface^[14] and the interface void can be eliminated with appropriate pressure,^[17] the poor wettability at the R/M interface led to a decrease in joint strength with increase

GUIFENG ZHANG, Associate Professor, and WEI SU, Graduate Student, are with the State Key Laboratory for Mechanical Behavior of Materials, Xi'an Jiaotong University, Xi'an 710049, P.R. China. Contact e-mail: gfzhang@mail.xjtu.edu.cn. AKIO SUZUMURA, Professor, is with the Department of Mechanical and Aerospace System Engineering, Tokyo Institute of Technology, Tokyo 152-8552, Japan.

Manuscript submitted July 26, 2014

Article published online February 10, 2016.

in volume fraction of reinforcement.^[7,15] For Al-25Cu-5Si-2Mg (wt pct) braze with a low melting range from 798 K (525 °C) to 808 K (535 °C), chloride flux (rather than fluoride flux) or relative high pressure (2 MPa) was recommended when brazing 15 vol pct SiC_p/6061Al in air or brazing 10 vol pct SiC_p/2024Al in vacuum, respectively, to achieve better wettability.^[18,19] In the wettability test using flux, the Al-28Cu-5Si-2Mg brazing filler metal could spread on a substrate of 15 vol pct SiC_p/6061 composite, but it failed to spread on the composite substrate containing 30 vol pct SiC particles.^[19]

As an alternative process to conventional soldering and brazing, transient liquid phase (TLP) bonding using an interlayer containing sufficient melting point depressant (MPD, eutectic former of Al), such as Cu,^[21–24] Ag,^[25] and Ni,^[26] can remove oxide film on the Al matrix *via* an undermining mechanism^[27–31] and can finally obtain an Al-based solid-solution bond seam after isothermal solidification and homogenization.^[32–34] However, poor wettability at the R/M interface and ceramic particle segregation at the center line of bond seam significantly limit the properties of TLP bonded joints. Of the two problems, poor wettability is more important than particle segregation because even if the particles can be distributed uniformly in the bond seam, poor wettability at the R/M interface will result in an interfacial gap between the ceramic particle and bond matrix, significantly damaging joint strength.

For counteracting particle segregation, many studies have been performed, in which thinner Cu foil^[23,24] and Al-Cu binary interlayer^[35] were suggested to reduce particulate segregation by limiting matrix dissolution width. Also, Ni or Sn was added in the Cu interlayer, preparing Cu/Ni/Cu sandwich foil^[36] and mixed Cu-Ni powder^[37] or Cu/Sn/Cu^[38] as modified interlayers to suppress particle segregation. Although the achieved joint efficiency for mixed Cu-Ni powder interlayer (84 pct of parent 13 vol pct SiC_p/6061Al) was much higher than that for the Cu/Ni/Cu stacked foil interlayer (68 pct), it was still lower than that obtained with a pure Cu interlayer.^[37] Because of the presence of a naked SiC particle on the fracture surface, one reason for such low joint efficiency was that the failure primarily occurred through decohesion at the SiC/M interface.^[37]

In recent years, some researchers succeeded in reinforcing bond seams by externally adding a ceramic particle into the monolithic interlayer. Yan *et al.* developed a SiC particle-reinforced Zn-4.6Al-3Cu (wt pct) filler metal to join 20 vol pct SiC_p/A356 composite at 693 K (420 °C) in air, and a dramatic increase in bond strength (~30 MPa) occurred as the ultrasonic vibration time exceeded 2 seconds because of the penetration of liquid Zn into the A356 substrate, partial melting of A356 matrix, and homogeneous distribution of particles with the aid of ultrasonic vibration.^[39] Cooke added nanoscale Al₂O₃ particles into 5- μ m-thick Ni coating (in 18 vol pct) and then increased joint shear strength by 20 MPa in TLP bonding of 15 vol pct Al₂O_{3p}/6061Al composite at the temperature of 873 K (600 °C) [which is slightly higher than Al-Ni-Si ternary eutectic temperature of 838 K (565 °C)] for 10 minutes in a vacuum.

The favorite shear strength was attributed to the formation of ternary Al-Ni-Si eutectic liquid, the nanoparticles arranged along grain boundary of bond matrix, and their pinning effect.^[40]

On the other hand, until now, a few studies on the development of an active filler metal for improving wettability have been reported. Weng and Chuang early stated that Sn10Ag4Ti (wt pct) active filler metal could wet the Al₂O_{3p}/6061Al composite well for the reason that the Sn10Ag4Ti filler metal begins to adhere to the Al₂O₃ particulate aligned along the joining surface above 873 K (600 °C).^[41] Lugscheider *et al.* developed an active solder of Sn91.8/Ag4/Ti4/Ga0.1/Ce0.1 to a wet silicon substrate in microsystem fabrication.^[42,43] Huang *et al.* added Ti powder (<3 wt pct) into a mixed Al-Si-SiC powder as an interlayer to improve the wettability of the SiC powder by the liquid Al-Si alloy formed by eutectic reaction in the powder interlayer. They claimed that a dense joining layer was formed for connecting the two SiC_p/6063 composites, and no obvious SiC segregation was found in the bond seam.^[44]

In recent years, the present authors' group has attempted to add active elements (which can react with ceramic reinforcement, *e.g.*, Ti, Zr, Li, or Mg) into a general Al-based brazing filler metal to improve the wettability at the R/M interface, and the TLP bonding process using the Ti-containing active interlayer is called active-TLP bonding (A-TLP) process by the present authors' group.^[45] For a high-volume-fraction SiC particle (70 vol pct)-reinforced A356 composite, it was found that dual-active elements of Mg and Ti are essential for improving the wettability at M/M and at R/M interfaces, respectively.^[46] For a low-volume-fraction SiC particle (10 vol pct)-reinforced A356 composite, it was found that Al-Cu-Ti ternary active interlayer can wet both A356 matrix and SiC particle, and it can produce a reinforcing phase of *in situ* small and dispersive Al-Si-Ti intermetallic phase within the TLP bond seam.^[47] For a medium-volume-fraction short alumina fiber (30 vol pct)-reinforced pure Al composite, in our previous study evaluating the wettability using the sessile drop method,^[48] it was found that the Al-12Si-1Ti active filler metal penetrated *in situ* into the composite substrate faster and covered Al₂O₃ short fiber closely, and a bare Al₂O₃ short fiber was difficult to observe on the substrate surface. For the common Al-12Si brazing filler metal, the interfacial gaps at the R/M interface could not be eliminated due to poor wettability.

Following our previous study on wettability,^[48] this work aims to further demonstrate the beneficial effect of adding Ti in trace levels into the interlayer on improving the microstructure and property of joints.

II. EXPERIMENTAL

The aluminum matrix composite used was fabricated by pressure casting,^[25] which consisted of pure Al matrix (to simplify analysis) and short ceramic fiber reinforcement with a medium volume fraction of 30 vol pct and an average size of 3.6 μ m in diameter and 140 μ m in length. The ceramic reinforcement consisting of 85 wt pct Al₂O₃ and 15 wt pct SiO₂ (see Figure 1) had

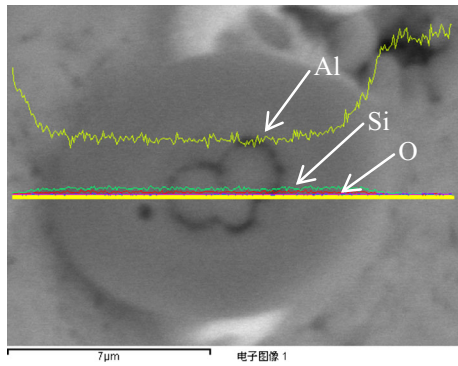


Fig. 1—EDS line scan analysis results showing the presence of both Si and Al in the chopped oxide fiber reinforcement.

a higher mole ratio of alumina to silica (~3:1) than typical mullite ($3\text{Al}_2\text{O}_3 \cdot 2\text{SiO}_2$), and then it was considered to be an alumina-based short fiber, denoted as $\text{Al}_2\text{O}_{3\text{sf}}/\text{Al}$. It was reported that the presence of SiO_2 layer on SiC surface formed by passive oxidation of SiC not only could be effective for prohibiting a direct contact between SiC and Al, but also it favored a reactive wetting between Al and SiC.^[49–51] Because of the pressure casting technique and the improved wettability between the reinforcement and pure Al matrix, the $\text{Al}_2\text{O}_{3\text{sf}}/\text{Al}$ composite exhibited a dense interface between the Al matrix and the short reinforcement fiber and a high tensile strength of 173 MPa.^[25] The shear strength of the as-cast $\text{Al}_2\text{O}_{3\text{sf}}/\text{Al}$ was measured as 89.3 MPa. The samples with different sizes ($15 \times 15 \times 1.8$ mm and $5 \times 5 \times 1.8$ mm) were polished using dry 600-grit silicon carbide paper, cleaned by ultrasonic vibration in acetone for 5 minutes, and then assembled in overlap configuration.

A series of 100- μm -thick active interlayer foils of Al-12Si- x Ti ($x = 0, 0.1, 0.5,$ and 1 wt pct) were developed by melting Al, Al-20Si and Al-5Ti master alloys at 1103 K (830 °C) for 30 minutes, followed by rapid solidification using rotating Cu wheel. Their microstructure, melting range and wetting behavior have been investigated and published elsewhere.^[48,52]

The schematic illustration of the bonding system is shown in Figure 2. TLP bonding using Al-12Si and Cu interlayer and A-TLP bonding using an active Ti-containing interlayer (Al-12Si- x Ti, $x = 0.1, 0.5,$ and 1 wt pct) were compared in terms of interfacial wettability, bond seam microstructure, shear strength, and fracture path to clarify the beneficial effect of Ti addition into traditional Al-based interlayer (or brazing filler metal) and to optimize the combination of the active interlayer composition with the bonding pressure. Each bonding was performed in flowing argon (4L minute^{-1}) at 883 K (610 °C) for 30 minutes under two pressure patterns, *i.e.*, a constant high pressure (1 MPa) like that used in general TLP bonding of metals and an initial high pressure (1 MPa) followed by a low pressure (0.015 MPa) after melting of the interlayer to avoid discharging of the melt for the poor wetting couple. It took 5 minutes to heat the samples from room temperature to the preset bonding temperature.

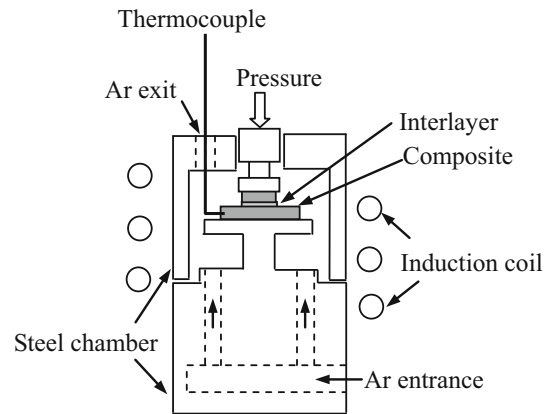


Fig. 2—Schematic of bonding apparatus.

At least four joint samples were prepared for each selected combination of parameters. Among them, three joint samples were used to evaluate joint strength by push-shear mode, and one joint sample was used to examine the microstructure. Backscattered electron (BSE) imaging was used to examine joint microstructure and fracture path, and energy-dispersive X-ray spectroscopy (EDS) was combined to investigate the diffusion result and newly formed phase. For a comparison, the popular interlayer of Cu foil with a thickness of 50 μm was also used at 853 K (580 °C) for 30 minutes to suppress particle segregation. Special attention was paid to the phenomena caused by Ti addition, including the ability to eliminate the interfacial gap at R/M interface, the distribution feature of the active element of Ti, and the phase constituent characterization of the bond seam.

III. RESULTS AND DISCUSSION

A. Joint Shear Strength for Different Interlayers and Pressure Patterns

Table I shows the variation of joint shear strengths depending on the Ti content and pressure pattern at 883 K (610 °C) for 30 minutes. For the effect of Ti addition on improving joint properties, it can be seen that with increasing the Ti content from 0 to 0.5 wt pct, the average joint shear strength increased from 60 MPa to 80 MPa for high pressure and from 75 to 89 MPa in the case of reducing pressure after melting of the interlayer. The results clearly confirmed that adding an appropriate amount of Ti (*e.g.*, trace level less than 1 wt pct) could significantly enhance the joint shear strength; namely, A-TLP bonding would be more effective over general TLP bonding for the composite containing medium volume fraction ceramic reinforcement. Unlike general TLP bonding of monolithic metal, only MPD (Si) is not enough to wet the entire interface because several ceramic reinforcements in the Al-MMC are difficult to be wetted by the Al-based interlayers. The increase in joint shear strength should be attributed primarily to the improvement in wettability by adding the active element Ti, especially at the R/M interface (see Section III-B).

Table I. Effect of Ti Content and Pressure on Joint Shear Strength

Interlayer (Weight Percent)	Pressure (MPa)	Shear Strength (MPa)			Average Strength (MPa)
		1	2	3	
Al-12Si	1	47	65	70	60
	0.015	74	75	76	75
Al-12Si-0.1Ti	1	66	74	77	73
	0.015	77	81	83	80
Al-12Si-0.5Ti	1	76	78	86	80
	0.015	87	89	90	89
Al-12Si-1Ti	1	47	47	54	50
	0.015	75	75	79	76
Cu*	1	42	35	44	40

*Bonding condition: 1 MPa × 30 min × 853 K (580 °C).

In contrast, it should be noted that although Al-12Si-1Ti exhibited more favorable wettability over Al-12Si in a previous study,^[48] the A-TLP joint prepared with Al-12Si-1Ti showed the lowest strength. The result showed that for a high Ti content, good wettability did not consequentially imply high properties in the couples, although isothermal solidification had been completed.^[48]

For the effect of reducing pressure after melting of the interlayer on improving joint properties, it can be seen that in this case, joint shear strength could be further improved by ~7 MPa for a Ti-containing active interlayer and ~16 MPa for common Al-12Si interlayer. Suzumura *et al.* succeeded in increasing the tensile strength of the joint of the Al₂O₃/Al composite brazed at 893 K (620 °C) for 200 seconds in a vacuum *via* reducing bonding pressure (from 4 to 2 MPa) and inserting a 0.3-mm-thick Al spacer to avoid discharging of the molten brazing filler metal of Al-12Si-1.5Mg (4N04, 0.3 mm in initial thickness).^[15] The improvement is effective for the composite containing low volume fraction short alumina fiber (10, 15, and 20 vol pct), compared with the case of 30 vol pct.^[15] The results by the author and Suzumura *et al.* showed that unlike TLP bonding of Al using Cu or Ag interlayer, for the poor wetting couple, the joint strength was sensitive to bonding pressure, and low pressure should be preferentially applied after melting of the interlayer to avoid expulsion of liquid phase, even for an active interlayer. The fact that the remaining liquid was beneficial to finally obtaining an enhanced joint suggested that there was a nonignorable incubation period for starting a wetting reaction. The presence of incubation time for a wetting reaction should be related to the presence of ceramic reinforcement. Also, a higher pressure before melting of interlayer is expected to create close contact early and widely between composite and interlayer in the solid state.^[25]

In particular, the maximum shear strength (88.6 MPa) could be obtained when using Al-12Si-0.5Ti active foil and reducing bonding pressure after melting of the interlayer. The maximum shear strength was quite close to that of the as-cast parent composites (89.3 MPa), reaching 99 pct joint efficiency. The result showed the importance of a suitable combination of Ti content and pressure pattern. In principle, retaining a molten active

interlayer in a required amount and for a required time (depending on volume fraction of ceramic reinforcement and incubation period) is essential for obtaining a sound joint.

B. Effect of Ti Addition and Pressure on Microstructure at Interface and Bond Seam

1. Interfacial microstructure evolution for interlayers with and without Ti

Figure 3 shows the difference in interfacial gap evolution behavior between the two cases using traditional Al-12Si and Al-12Si-1Ti active interlayers during different holding periods (ranging from 5 seconds to 10 minutes) at 883 K (610 °C) under 1 MPa pressure. The improvement in wettability by adding Ti as active element can be demonstrated by the following two facts: rapid disappearance of interfacial gap and the presence of remaining interlayer at anywhere even under high pressure.

It is worth noting that in the early stages of the brazing process, the interfacial gap at M/M microinterfaces for Al-12Si-1Ti foil could be eliminated much faster than that for Al-12Si foil. For example, at 500× magnification, the interfacial gap at M/M microinterfaces for Al-12Si-1Ti foil disappeared in approximately 5 seconds (Figure 3(a)), whereas for Al-12Si foil, the interfacial gap at M/M microinterfaces disappeared in approximately 10 minutes (Figure 3(h)). In the previous work, after the wetting test using the sessile drop method in flowing argon without any pressure,^[48] the amount of the residue of molten Al-12Si was more than that of Al-12Si-1Ti, showing that Al-12Si-1Ti was able to penetrate into Al matrix faster than Al-12Si. The significant reduction in the total time for eliminating interfacial gap indicated that the liquid Ti atoms accelerated the interfacial reaction at most M/M microinterfaces like Mg^[15,53] and improved the wettability at R/M microinterfaces to some extent. For Al-12Si brazing filler metal, the presence of oxide film on the molten filler metal Al-12Si surface should be primarily responsible for the long incubation period for wetting, although the reinforcement contained SiO₂.^[54] For Al-12Si-1Ti interlayer, only Ti can react with an ultrathin oxide film, but it cannot entirely remove the

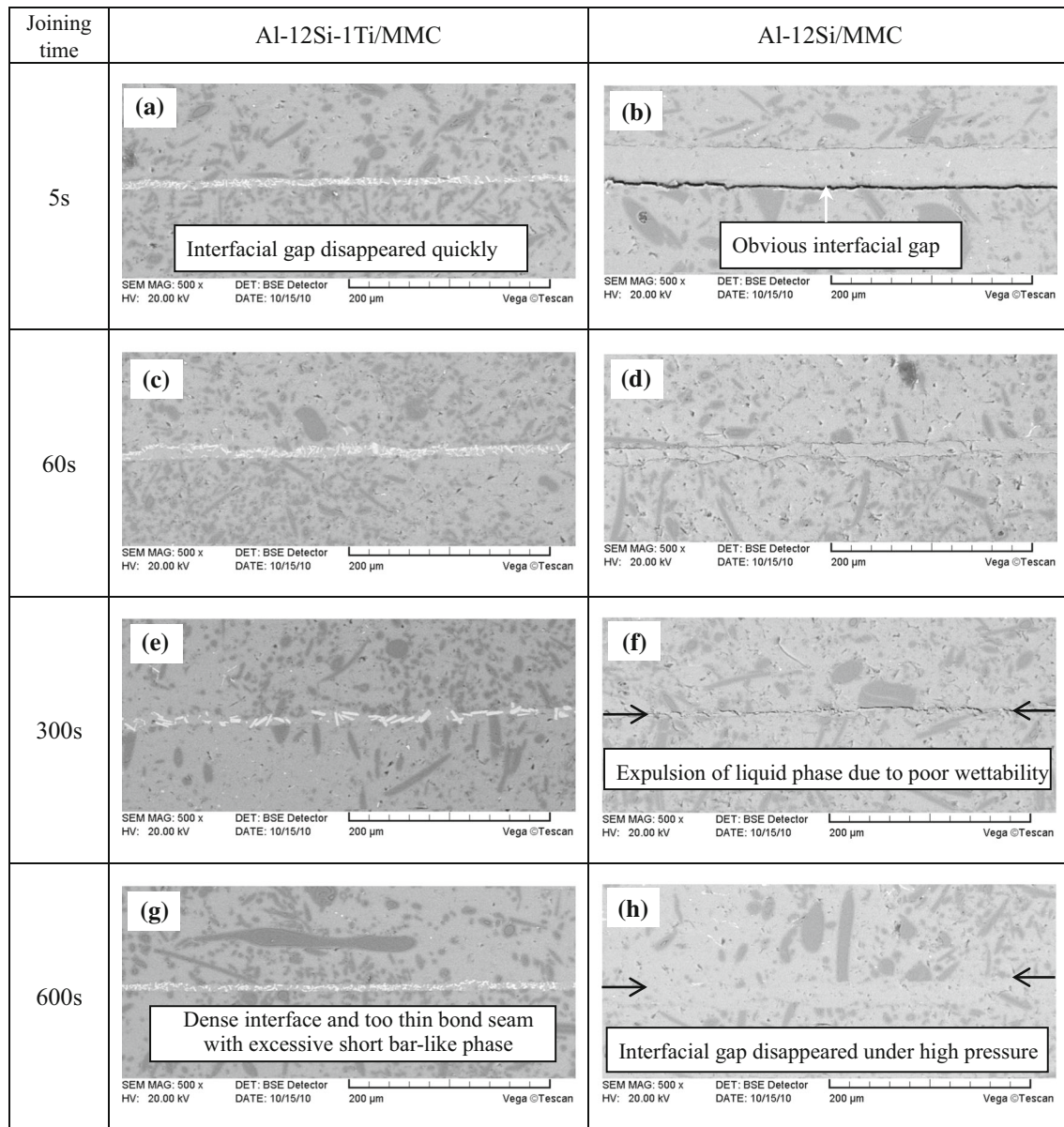


Fig. 3—Comparison of evolution of the interfacial gap in the early stage of the joint formation using the interlayers with and without Ti under high pressure of 1 MPa at 883 K (610 °C).

oxide film. In contrast, Si as MPD with a relatively high content can dissolve the Al matrix significantly, achieving wetting at all M/M microinterfaces. So, the combination of Ti (as active element with a trace level content) and Si (as MPD with a relatively high content) could remove oxide film rapidly and extensively in the A-TLP bonding process. Namely, active Ti atoms in the molten state can react with oxide films at the surfaces of both the molten braze and solid matrix, disrupting the integrity of the oxide films, rapidly establishing initial diffusion path for MPD of Si, and subsequently promoting wetting at the M/M microinterface.

In the A-TLP bonding process, the establishment of an initial diffusion path for MPD does not rely only on the cracking of the oxide film caused by the mismatch in coefficient of thermal expansion between metal and its oxide film. The active element Ti could also play a prior

and chemical role in disrupting oxide film and establishing initial diffusion path for MPD at M/M micro-interface. The important feature of active element would be valuable for joining Al-MMCs containing medium and high volume fraction ceramic reinforcement.

The other evidence for improvement in wettability was that the molten active interlayer Al-12Si-1Ti was difficult to extrude completely from the interface anywhere for any period under high pressure. For Al-12Si filler metal, the unbonded areas without filler metal were observed sometimes, especially at the R/M microinterface with relatively large ceramic particles. The poor wettability and resultant long incubation period should be responsible for extrusion of the liquid phase from faying surfaces.

On the other hand, large numbers of Ti-containing short bar-like intermetallic compounds (IMCs, white

phase in Figure 3) were formed *in situ* in the bond seam for Al-12Si-1Ti layer, and their size could reach the bond seam thickness. Moreover, it seems that the number of the Ti-containing short bar-like IMCs did not decrease with increasing holding time. The results suggested that Ti was hard to diffuse into Al matrix, and then excessive Ti tended to form aluminide in bond seam, because (I) Ti has little solubility in Al^[55] and (II) Ti is a melting point increaser (MPI) for Al rather than a MPD.^[47,48]

2. Final microstructure under high pressure

Figure 4 shows the final microstructure using different interlayers of Al-12Si- x Ti ($x = 0, 0.1, 0.5, \text{ and } 1$ in wt pct) under high pressure of 1 MPa at 883 K (610 °C) for 30 minutes. No particle segregation, void, and reaction products at the R/M interface were observed for any of the interlayers. Seemingly, it is hard to distinguish the difference in wetting behavior at the R/M interface. However, it is easy to differentiate the following aspects for the interlayer with and without Ti: (I) the

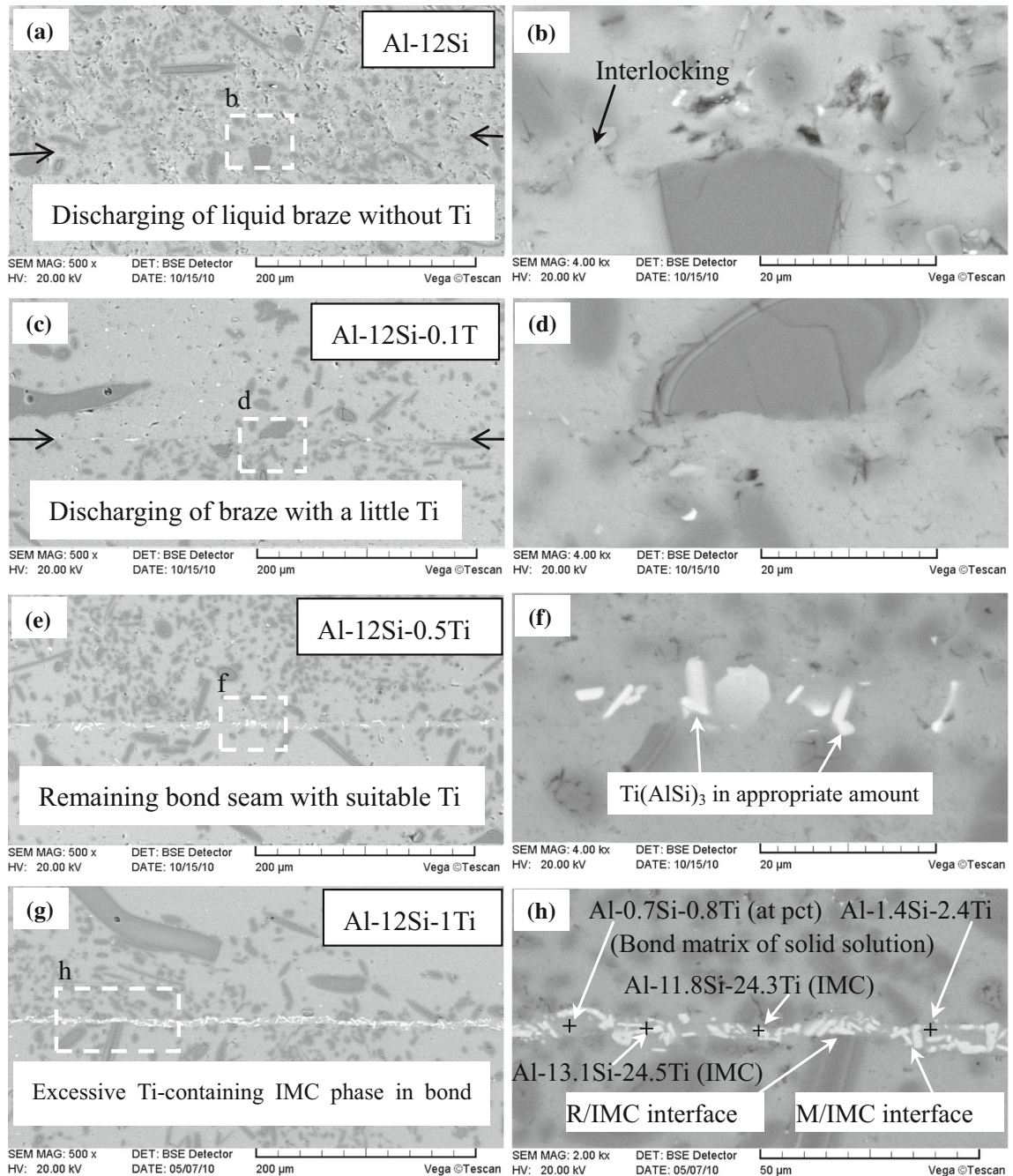


Fig. 4—Microstructures of joints prepared with different interlayers of Al-12Si- x Ti ($x = 0, 0.1, 0.5, \text{ and } 1$ wt pct) under high stress of 1 MPa at 883 K (610 °C) for 30 min: 0 Ti (a, b); 0.1 Ti (c, d); 0.5 Ti (e, f); and 1 Ti (g, h).

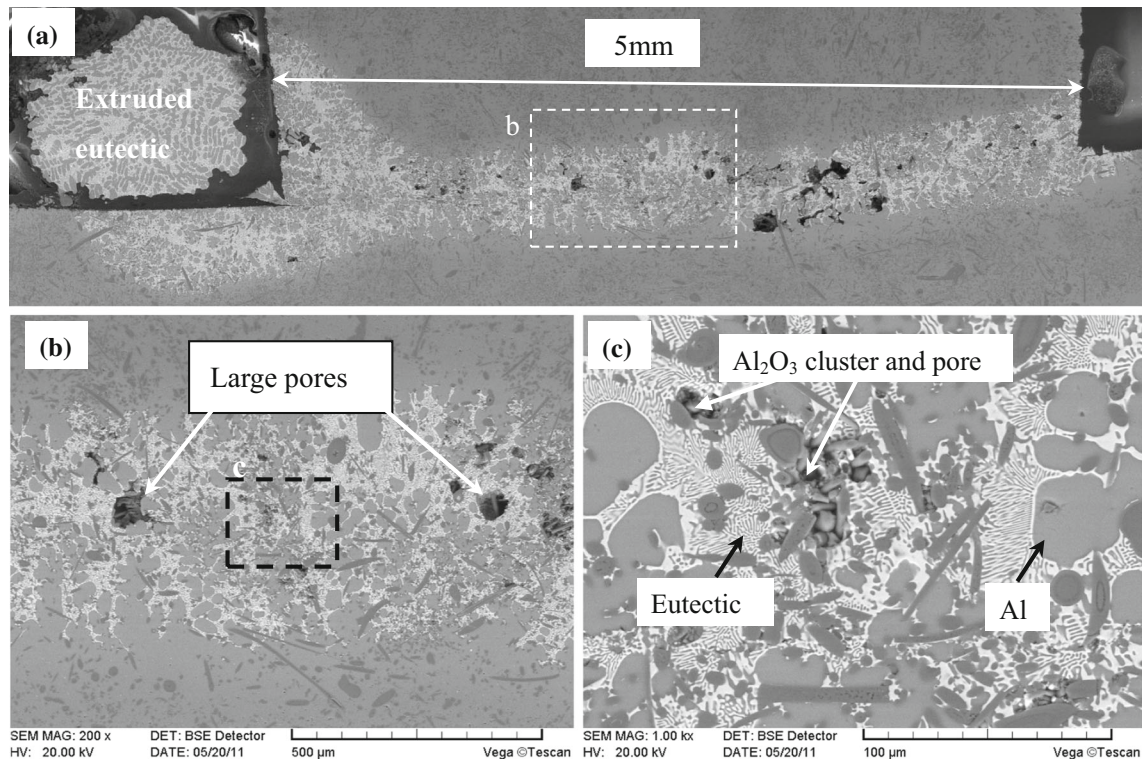


Fig. 5—BSE images of microstructure of the general TLP bonded joint using a popular Cu foil interlayer under the condition of 1 MPa \times 30 min \times 853 K (580 °C) showing the disappearance of M/M interface (a), brittle eutectic-containing matrix and large pores (b), and defects including short fiber cluster and small pores caused by poor wettability at the R/M interface (c).

bond seam thickness, (II) the kinds of phases in the bond seams, and (III) the resultant types of interface between the bond seam and the parent composite.

For the Al-12Si interlayer, the residual thickness of the bond seam was decreased from initial 100 μm to about 0 μm . Such an evidence of discharging of the molten Al-12Si out of the interface indicated that (I) the incubation time to start wetting reaction with Al matrix could not be reduced by pressure, although the pressure was able to break oxide film on the molten Al-12Si braze, and (II) a very thin layer of residual molten Al-12Si would isothermally solidify rapidly, terminating the wetting reaction at some liquid/solid microinterfaces.^[15] However, no gap was observed at the R/M interface for the Al-12Si interlayer, even at 4000 times magnification. It should be attributed to creep deformation and interlocking at M/M interface at 883 K (610 °C) under 1MPa and minor reaction at the R/M interface. The latter could be possible because the presence of SiO₂ in the reinforcement can significantly decrease the wetting reaction temperature from 1223 K (950 °C) for Al/Al₂O₃ system to 973 K (700 °C) for Al/SiO₂ system, facilitating the wetting at the R/M interface.^[54] However, the low bonding temperature of 883 K (610 °C) limited the reaction degree, leading to limited wetting at the R/M interface without detectable reaction products. Moreover, the possible reaction products of both Al₂O₃ and Si are difficult to distinguish from original ceramic phase and Al matrix by the BSE image. Based on the discharge of molten braze, low joining temperature, and poor spreading behavior on the

composite substrate,^[14] it can be deduced that Al-12Si could not reliably wet the alumina-based reinforcement.

For Al-Si-Ti interlayer, the final microstructure can be characterized as follows: (1) no interfacial gap was observed and the active interlayer was not completely discharged, although the thickness of the bond seam was significantly decreased from 100 to 5 μm under high pressure; (2) several short bar-like Ti-containing IMC phases (5 to 10 μm in length and \sim 2 μm in thickness) *in situ* precipitated within the bond seam; (3) the volume fraction of the newly formed Ti-containing IMC phase increased with increasing Ti content, reaching a level much more than 30 vol pct, especially for the Al-12Si-1Ti interlayer; (4) the *in situ* formed Ti-containing IMC phase was also difficult to extrude from the joint interface under the bonding pressure; and (5) Ti was difficult to detect in the composite adjacent to the surface. Although the reaction products at the R/M interface for any of the Ti-containing active interlayers were not detected, the presence of residual bond seam and the dense bond/composite interface confirmed that Al-12Si-1Ti had more favorable wettability over Al-12Si. Moreover, the presence of Ti-containing IMC phase within the bond seam and the absence of Ti in the composite adjacent to the surface showed that liquid Ti atoms tended to remain in the bond seam rather than to diffuse into solid Al matrix. The distribution feature of Ti could be explained by the little solubility of Ti in Al, the slow diffusion rate in Al matrix,^[55] the bonding temperature lower than the melting point of Al matrix, and the precipitation nature

of Ti in the form of aluminide from liquid phase during isothermal solidification.^[47]

The EDS point analysis results showed that the Al-Si-Ti IMC phase belonged to $\text{Ti}(\text{AlSi})_3$ phase with low Si content, which was less than 15 wt pct.^[56] In recent years, aluminide particles such as NiAl_3 , FeAl_3 , and TiAl_3 were believed to be useful reinforcements for aluminum alloys to increase specific strength, specific modulus, or wear resistance at both ambient and elevated temperatures,^[55,57] and compared with most other aluminum-rich intermetallics, Al_3Ti is very attractive because it has a high melting point of 1623 K (1350 °C) and a relatively low density (3.4 g/cm³).^[55] Because the current Ti-containing IMC phase was successfully dispersed in the bond seam and had a similar size to the original Al_2O_3 short fiber reinforcement and a dense interface with the bond matrix (being solid solution after isothermal solidification and homogenization), it could act as an *in situ* reinforcement within the bond seam.^[47]

Although the Al-Si-Ti phase can be considered to be a new kind of reinforcement,^[56] it should be noted that the presence of large amounts of the Al-Si-Ti phase gave rise to an interface between the ceramic reinforcement and the Al-Si-Ti phase (denoted as the R/IMC interface). The R/IMC interface should be weak because the Al-Si-Ti phase would crystallize from the liquid phase through concentration-precipitation-termination-engulfment of Ti with the aid of Si diffusion into Al matrix during isothermal solidification^[47] rather than nucleate at the ceramic reinforcement. Similarly, an interface between Al matrix and the Al-Si-Ti phase would present (denoted as the M/IMC interface). Thus, in the A-TLP joint produced with Al-12Si-1Ti, the four kinds of interfaces are M/M, R/M, M/IMC, and R/IMC.

Although the M/M and R/M were bonded intimately (no void at 4000 times magnification), the presence of M/IMC and R/IMC interfaces would counteract the effect of dense bonding at M/M and R/M interfaces because some of the strong M/M and R/M interfaces were replaced by numerous weak M/IMC and R/IMC interfaces, respectively, leading to the fracture along the M/IMC and R/IMC interfaces (Referring to Figure 8(h) showing the fracture path and Figure 9(b) showing the fracture surface in Section III-C).

Because of the more favorable wettability at the R/M interface and the presence of the *in situ* formed $\text{Ti}(\text{AlSi})_3$ within the bond seam in a medium amount, the A-TLP joint using Al-12Si-0.5Ti exhibited the maximum shear strength. In contrast, for the Al-12Si-1Ti interlayer, although it exhibited better wettability over other interlayers, the presence of excessive short bar-like Ti-containing IMC phase resulted in many weak M/IMC and R/IMC interfaces, which led to a lower joint strength than that using Al-12Si. The acceptable joint shear strength for Al-12Si should benefit from the limited wetting at some rough M/M interfacial areas and mechanical interlocking at many M/M and R/M interfaces under high pressure.

Figure 5 shows the popular TLP-bonded joint using 50- μm -thick Cu foil interlayer at 853 K (580 °C) for 30 minutes under a pressure of 1 MPa. The wetting at the M/M interface has been achieved well by the eutectic reaction, but the resultant eutectic layer was too thick, reaching 500 μm because of the deep dissolution reaction. For this composite with medium Al_2O_3 volume fraction (generally produced by pressure casting), although no evident particle segregation was observed, the newly formed thick Al-Cu eutectic liquid phase was difficult to extrude even under higher pressure.

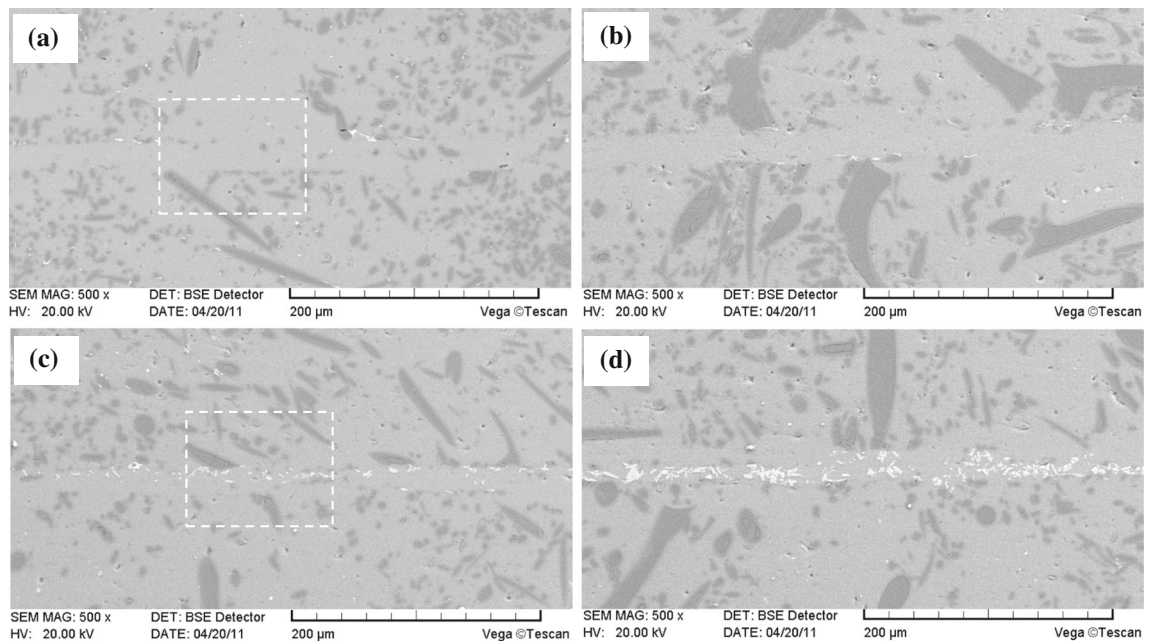


Fig. 6—Microstructures of joints prepared under low pressure of 0.015 MPa [883 K (610 °C) × 30 min] showing the increase in bond seam thickness and the decrease in volume fraction of the *in situ* precipitated Ti-containing IMC phase within the bond seam compared with the case under 1 MPa: (a) 0 pct Ti, (b) 0.1 pct Ti, (c) 0.5 pct Ti, and (d) 1 pct Ti.

Additionally, in the vicinity of the interface, the presence of Al_2O_3 cluster and pores within the cluster demonstrated that the molten Cu exhibited poor wettability. Both the thick eutectic region and pore defects degraded the joint strength.

3. Final microstructure under low pressure

Figure 6 shows the microstructures of joints prepared using Al-12Si- x Ti ($x = 0, 0.1, 0.5,$ and 1 in wt pct) interlayers under low pressure of 0.015 MPa after melting of the interlayers. Like the microstructure of joints brazed under 1 MPa, no particle segregation, void, or reaction products at the R/M interface were observed for any of the interlayers, and the Al-Si-Ti IMC phase also existed within the bond seam. The low pressure resulted in the following beneficial effects. First, although the thickness of the bond seam changed from initial value of 100 to ~ 25 μm , the final thickness was greater than that under high pressure of 1 MPa by ~ 20 μm . Second, the volume fraction of the *in situ* precipitated Ti-containing IMC phase within the bond seam decreased compared with that prepared under high pressure. The former was beneficial to (1) avoiding excessive discharging of the molten interlayer, thus achieving the dissolution of Al matrix and wetting at the M/M interface; and (2) reducing the volume fraction of the *in situ* precipitated Ti-containing IMC phase within

the bond seam. The latter was beneficial to decreasing the number of the M/IMC and R/IMC interfaces and then reducing the discontinuity in mechanical property at the final interface between the bond seam and composite.

The microstructure of the A-TLP joints using Al-12Si-0.5Ti under 0.015 MPa, which exhibited the maximum shear strength of 88.6 MPa (99 pct of 89.3 MPa of the as-cast $\text{Al}_2\text{O}_3/\text{Al}$ composite), was specifically examined in higher magnification, as shown in Figure 7. Even at high magnification of 2000 and $40,000$ times, no void was observed at the R/M interface as shown in Figures 7(a) and (b), indicating that the active Ti could improve the wettability at the R/M interface, although Ti was not detected at the R/M interface in the current work. For the *in situ* precipitated Ti-containing IMC phase within the bond seam, the EDS point analysis result showed that it had a composition of Al-18.6Ti-10.9Si (at. pct), so the IMC phase can be identified as $\text{Ti}(\text{AlSi})_3$, *i.e.*, a logogram of $\text{Ti}(\text{Al}_{1-x}\text{Si}_x)_3$ with small Si content, $0 \leq x \leq 0.15$.^[56] The $\text{Ti}(\text{Al}_{1-x}\text{Si}_x)_3$ phase has been demonstrated by Zeren and Karakulak to have outstanding wear resistance in Al-Si- x Ti cast alloy.^[56] Because (1) the Ti-containing IMC phase was so small, namely 2 to 5 μm in length and 1 μm in thickness (much smaller than short alumina fiber reinforcement) and dispersed uniformly, and (2) no

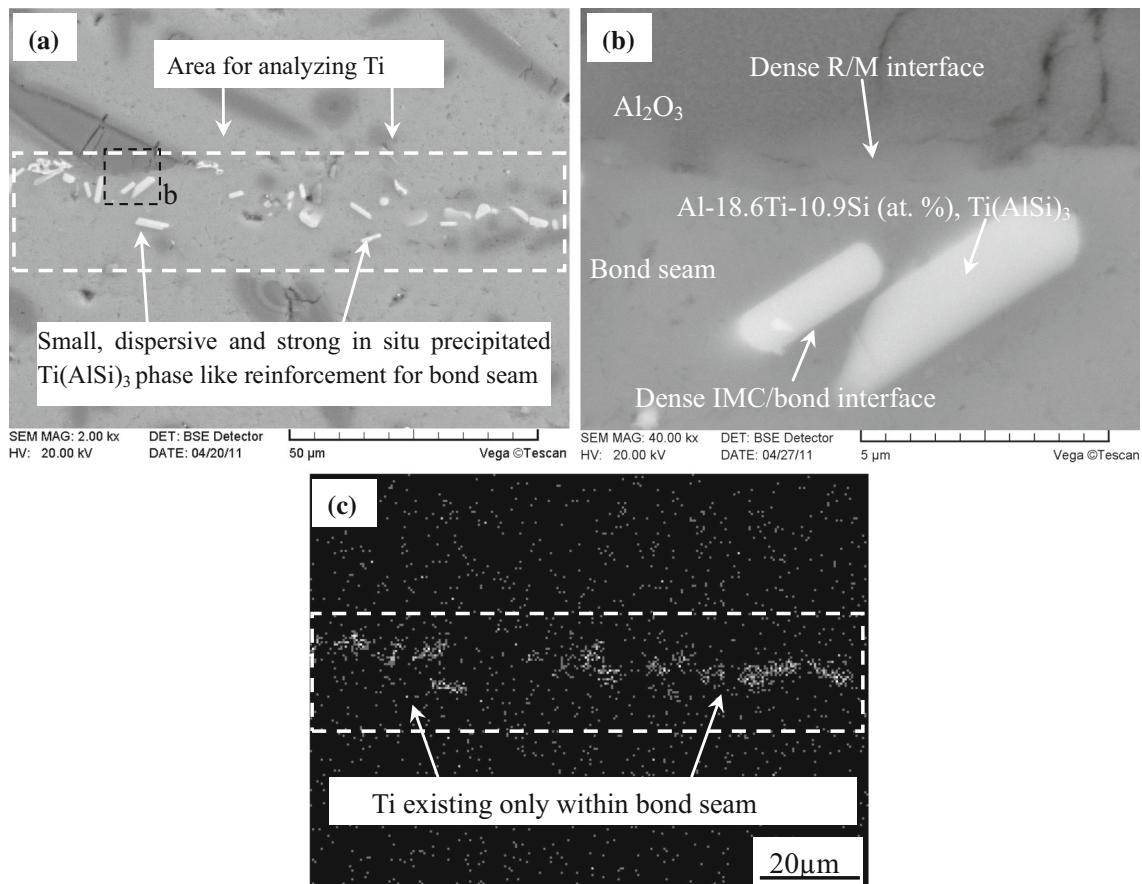


Fig. 7—Detailed microstructure of the A-TLP joint using Al-12Si-0.5Ti under low pressure showing dense R/M interface and the *in situ* precipitated Al-Si-Ti IMC phase (being small and dispersed) within the bond seam of solid-solution matrix after isothermal solidification.

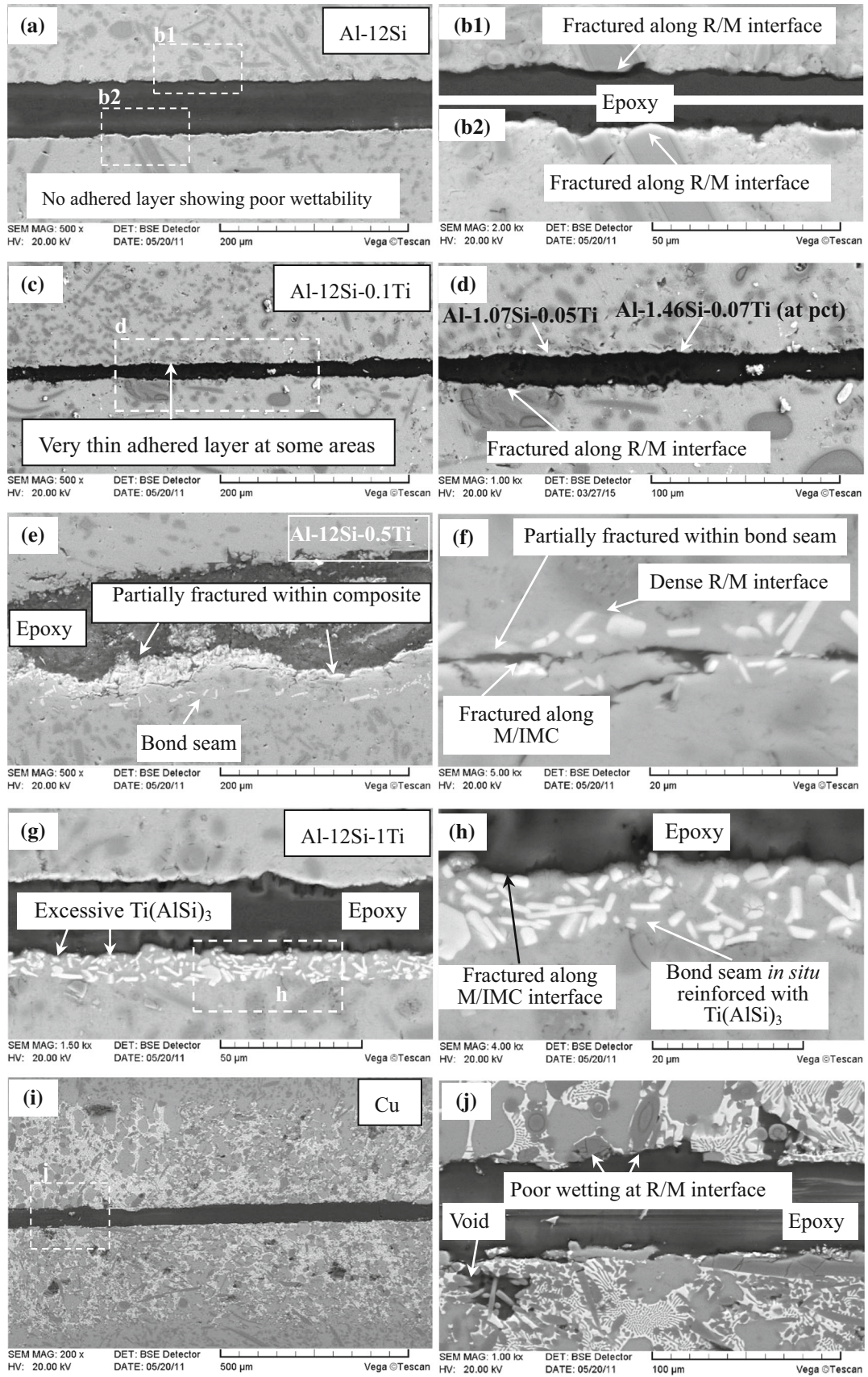


Fig. 8—Fracture path in the joints prepared under the condition of 883 K (610 °C) × 30 min × 1 MPa using different interlayers: (a, b) Al-12Si, (c, d) Al-12Si-0.1Ti, (e, f) Al-12Si-0.5Ti, (g, h) Al-12Si-1Ti, and (i, j) Cu.

void was observed at the IMC/bond seam matrix, the short IMC phase can act as an *in situ* reinforcement for bond matrix, which had become solid solution with little Si after isothermal solidification. Such an improvement in interface microstructure and the enhanced bond seam by the small, dispersed, and appropriate Ti-containing IMC phase (*in situ* precipitated) made the strength of the A-TLP joints higher.

C. Fracture Behavior

Besides joint microstructure, the effect of Ti addition on improvement of the joint shear strength can be also explained from the viewpoint of the joint fracture path, even under the high pressure of 1 MPa. As shown in Figure 8, there were four types of joint fracture paths depending on the Ti content: (1) flat and straight fracture path along the initial surface of the composite substrates without adhesion of interlayers of Al-12Si and Al-12Si-0.1Ti, (2) along the interface between enhanced bond seam and the Al-MMC for Al-12Si-1Ti, (3) mixed fracture path, within the matrix and/or bond seam of solid solution, for Al-12Si-0.5Ti, and (4) within the brittle Al-Cu eutectic matrix containing short fiber clusters and pores for Cu foil. The results demonstrated that an appropriate addition of Ti in interlayers can improve the mechanical performance of joints by changing the fracture path from completely along initial interface to partially into the bond seam or the matrix.

In particular, it should be noted that in the joint prepared using Al-12Si-1Ti, no crack initiation and propagation occurred within the bond seam, showing that the bond seam was significantly reinforced by the newly *in situ* formed $Ti(AlSi)_3$ phase. To understand the effect of the newly *in situ* formed $Ti(AlSi)_3$ phase on joint property and fracture behavior, the fracture surface of the joint using Al-12Si-1Ti was examined, as shown in Figure 9. Numerous short bar-like Al-Si-Ti phases with smooth surface could be seen on the adhered layer. The smooth surface of the Al-Si-Ti phase

showed that the excessive newly formed Al-Si-Ti phase had negative effects, resulting in a fracture along the M/IMC or R/IMC interfaces.

When reducing pressure after melting of the interlayer, the fracture path can be improved to some extent. For Al-12Si, the filler metal could be retained as shown in Figure 10. The low pressure prevented the filler metal from discharging, resulting in a longer period to react with Al matrix at the M/M interface and sound M/M interface. As a result, the joint shear strength was improved by 8 MPa more than that under high bonding pressure. However, the limited increase in shear strength, straight fracture path, and numerous bare ceramic reinforcements on the fracture surface suggested that the Ti-free Al-12Si interlayer was unable to improve the wettability at R/M even for a longer interacting time under low pressure. For the A-TLP joint produced with an Al-12Si-0.5Ti active interlayer under low pressure, three types of favorite fracture modes appeared, as shown in Figure 11. In mode I, fracture occurred within the composite as shown in Figure 11(a); this type of fracture mode accounted for approximately 13 pct of total fracture path. In mode II, fracture took place in the bond seam as shown in Figure 11(b) and accounted for 27 pct of the whole fracture path. In mode III, fracture happened along the interface between the composite and the bond seam newly formed through matrix dissolution and isothermal solidification, which accounted for 60 pct.

Clearly, mode I and mode II together accounted for approximately 40 pct of the whole cross-section of the tested joint, indicating that the interface bonding strength at the 40 pct region of interface was superior to that of the solid-solution bond seam matrix and/or the parent composite. It can be seen from Figure 11(c) that the Al_2O_3 short fiber was pulled apart from the composite because of the high strength at the R/M interface. The results demonstrated that the active Ti could improve the bonding at R/M partly. In particular, it should be emphasized that the fracture path for Al-12Si-0.5Ti active interlayer could partially propagate

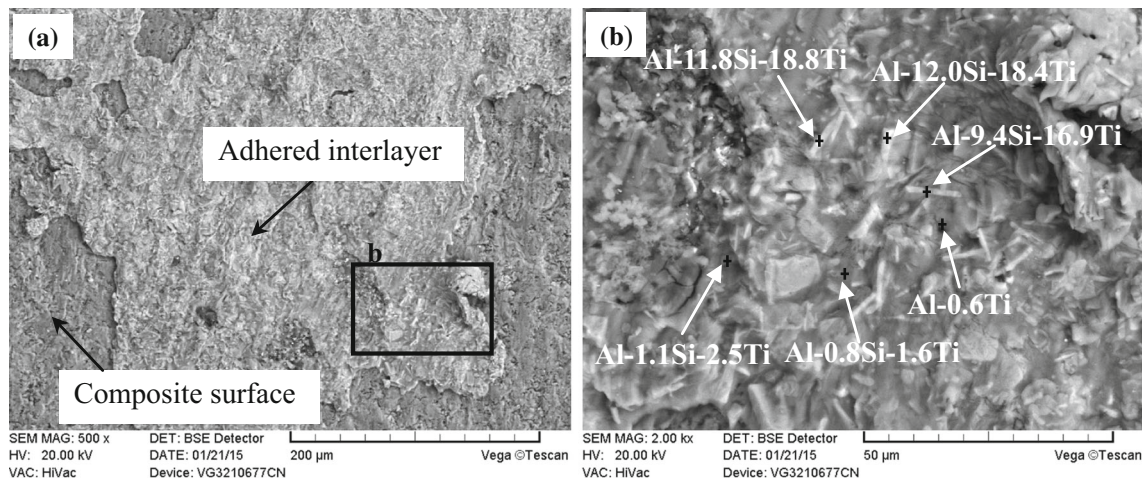


Fig. 9—Fracture surface of the A-TLP joint prepared with Al-12Si-1Ti showing the fracture path along the interface between bond seam and composite (a) and the presence of numerous newly formed short bar-like Al-Si-Ti phase with smooth surface on fracture surface (b).

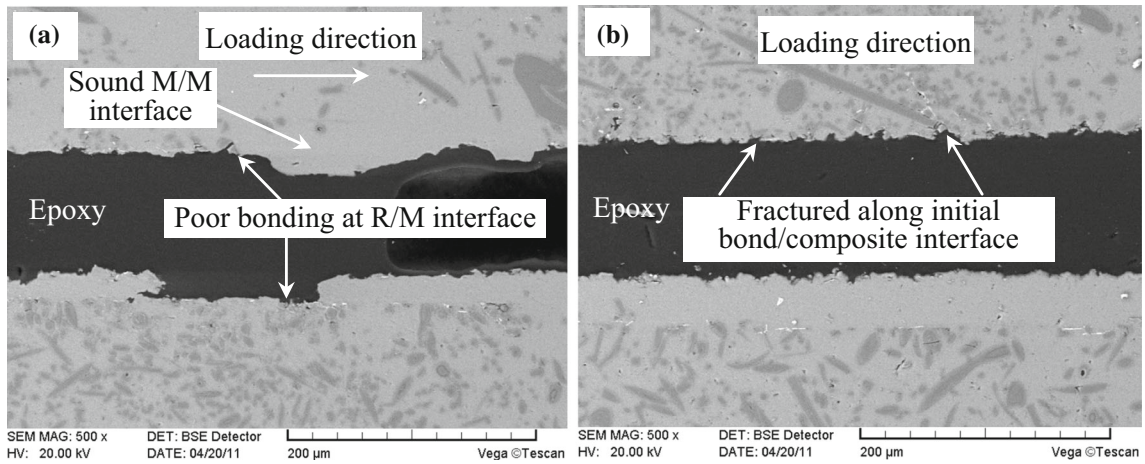


Fig. 10—BSE images of the fracture path in the joints prepared under the condition of 883 K (610 °C) × 30 min × 0.015 MPa using Al-12Si foil interlayer showing favorable joining at the M/M interface and poor joining at the R/M interface.

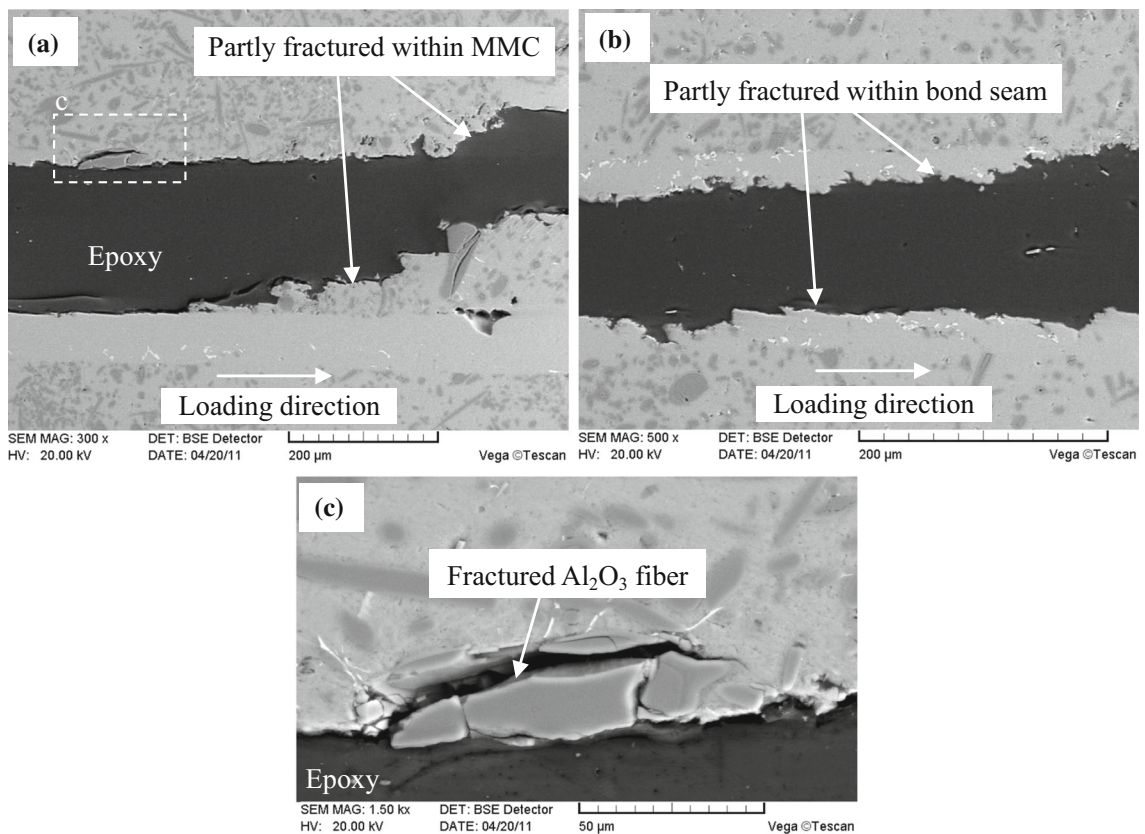


Fig. 11—BSE image of partial favorite fracture paths in the joint using Al-12Si-0.5Ti foil under low pressure showing different fracture modes: (a) within the composite and (b) within bond seam of solid-solution matrix. (c) A special example of strong interfacial bonding at R/M interface leading to fracture of the Al_2O_3 short fiber reinforcement.

into the $\text{Al}_2\text{O}_{3\text{sf}}/\text{Al}$ composite, indicating that both the interface joining and bond seam were enhanced well by improving wettability and the presence of *in situ* Al-Si-Ti phase, respectively. Moreover, reducing the pressure after melting of the interlayer could further improve the joint shear strength by avoiding liquid discharging during the incubation period, prolonging the liquid/solid reacting time for wetting and forming small and dispersive Ti-containing phase as *in situ*

reinforcement with appropriate volume fraction in the bond seam.

IV. CONCLUSIONS

To optimize both the interlayer composition design route and joining parameters for TLP bonding of the $\text{Al}_2\text{O}_{3\text{sf}}/\text{Al}$ composite, the A-TLP bonding using

Al-12Si- x Ti ($x = 0, 0.1, 0.5, \text{ and } 1$) system active fillers was performed under different pressures. By comparing the joint microstructure, shear strength, and fracture behavior, the conclusions can be summarized as follows:

1. The improvement in wettability by adding Ti as active element were confirmed by reduction of expulsion of liquid interlayer (reduced to $5 \mu\text{m}$ under 1 MPa and $25 \mu\text{m}$ under 0.015 MPa), elimination of interfacial gap, higher shear strength (by ~ 15 MPa), and favorable fracture path (partially through bond seam and the composite).
2. The added Ti was difficult to detect in the composite adjacent to the interface, and it tended to precipitate *in situ* within the bond seam in the form of short bar-like Al-Si-Ti IMC phase of $\text{Ti}(\text{AlSi})_3$ with a small Si content. The nature of small size ($\sim 5 \mu\text{m}$) and dispersive distribution of the *in situ* precipitated $\text{Ti}(\text{AlSi})_3$ IMC phase suggested that it could act as an *in situ* formed reinforcement for the bond seam matrix of solid solution after isothermal solidification. So, both the interfacial bonding and bond seam were enhanced by adding Ti in trace levels (0.5 wt pct).
3. The remaining Al-12Si liquid was finally able to increase joint shear strength, showing that there was an incubation period for wetting. Unlike popular TLP bonding using a Cu interlayer, when using an interlayer with a melting point lower than bonding temperature for joining Al-MMCs with poor wettability, reducing bonding pressure after melting of the interlayer was beneficial to the holding melt, prolonging the dissolution period of Al matrix, dispersing the *in situ* precipitated $\text{Ti}(\text{AlSi})_3$ IMC phase, and further improving joint shear strength.
4. Although high Ti addition (1 wt pct) could significantly improve the wettability and enhance the bond seam matrix, the joint shear strength decreased because of the presence of excessive M/IMC and R/IMC interfaces.
5. The maximum shear strength of 88.6 MPa, which is extremely close to that of the as-cast composite of 89.3 MPa (up to 99 pct efficiency), was obtained when using the active interlayer containing medium Ti content (0.5 wt pct) and a low pressure after melting interlayer (0.015MPa). In principle, retaining molten active interlayer in a required amount and for a required time (depending on volume fraction of ceramic reinforcement and incubation period) is essential to obtaining sound joint.

ACKNOWLEDGMENTS

The current research was supported by the National Science Foundation of China (Nos. 51275390 and 50875199) and partially supported by China Scholarship Council (CSC). The first author also greatly acknowledges Professor Yasuo Takahashi at Joining and Welding Research Institute, Osaka University, Japan, for his kind support at the manuscript preparation stage.

OPEN ACCESS

This article is distributed under the terms of the Creative Commons Attribution 4.0 International License (<http://creativecommons.org/licenses/by/4.0/>), which permits unrestricted use, distribution, and reproduction in any medium, provided you give appropriate credit to the original author(s) and the source, provide a link to the Creative Commons license, and indicate if changes were made.

REFERENCES

1. A. Ureña, M.D. Escalera, and L. Gil: *Compos. Sci. Technol.*, 2000, vol. 60, pp. 613–22.
2. D. Storjohann, O.M. Barabash, S.S. Babu, S.A. David, P.S. Sklad, and E.E. Bloom: *Metall. Mater. Trans. A*, 2005, vol. 36A, pp. 3237–47.
3. M.B.D. Ellis: *Int. Mater. Rev.*, 1996, vol. 41, pp. 41–58.
4. Y.C. Lei, H.L. Xue, W.X. Hu, Z.Z. Liu, and J.C. Yan: *Sci. Technol. Weld. Join.*, 2011, vol. 16 (7), pp. 575–80.
5. D. Wang, Q.Z. Wang, B.L. Xiao, and Z.Y. Ma: *Mater. Sci. Eng. A*, 2000, vol. 589, pp. 271–74.
6. A. Ureña, J.M.G. De Salazar, M.D. Escalera, and M.I. Fernandez: *Weld. J.*, 1997, vol. 76 (2), pp. 92s–102s.
7. XP Zhang, GF Quan, and W Wei: *Compos. Part. A*, 1999, vol. 30 (6), pp. 823–27.
8. A. Suzumura and Y.J. Xing: *Prepr. Natl. Meet. JWS*, 1994, vol. 55, pp. 282–83.
9. A. Ureña, L. Gil, E. Escriche, J.M. Gomez de Salazar, and M.D. Escalera: *Sci. Technol. Weld. Join.*, 2001, vol. 6 (1), pp. 1–11.
10. J.C. Yan, H.B. Xu, L. Shi, X.H. Wang, and S.Q. Yang: *Sci. Technol. Weld. Join.*, 2008, vol. 13 (8), pp. 760–64.
11. Z.W. Xu, J.C. Yan, and S.Q. Yang: *Mater. Sci. Eng. A*, 2006, vol. 415A (1–2), pp. 80–86.
12. H.B. Xu, Q.X. Xing, Y.L. Zeng, Y. Luo, and C.H. Du: *Sci. Technol. Weld. Join.*, 2011, vol. 16 (6), pp. 483–87.
13. W.P. Weng and T.H. Chuang: *Metall. Mater. Trans. A*, 1997, vol. 28A, pp. 2673–82.
14. A. Suzumura, Y. Xing, K. Takahashi, and T. Onzawa: *Prepr. Natl. Meet. JWS*, 1993, vol. 52, pp. 166–67.
15. A. Suzumura, M. Matsumoto, and Y. Xing: *Prepr. Natl. Meet. JWS*, 1996, vol. 59, pp. 262–63.
16. A. Suzumura, Y. Xing, and K. Takahashi: *Prepr. Natl. Meet. JWS*, 1993, vol. 53, pp. 326–27.
17. H. Kokawa, K. Mitsuzuka, and T. Kuwana: *Prepr. Natl. Meet. JWS*, 1993, vol. 52, pp. 176–77.
18. J.S. Zou, R.Q. Xu, Q.Z. Zhao, and Z. Chen: *China Weld.*, 2003, vol. 12 (2), pp. 107–11.
19. J.S. Zou, R.Q. Xu, Q.Z. Zhao, and Y.S. Han: *Mater. Dev. Appl.*, 2003, vol. 18 (4), pp. 5–12.
20. J. Niu, X. Luo, H. Tian, and J. Brnic: *Mater. Sci. Eng. B*, 2012, vol. 177 (19), pp. 1707–11.
21. T. Enjo, K. Ikeuchi, Y. Murakami, and N. Suzuki: *Trans. JWRI*, 1987, vol. 16 (2), pp. 285–92.
22. R. Klehn and T.W. Eagar: *WRC Bull.*, 1993, vol. 385, pp. 1–26.
23. Z. Li, Y. Zhou, and T.H. North: *J. Mater. Sci.*, 1995, vol. 30 (12), pp. 1075–82.
24. A.A. Shirzadi and E.R. Wallach: *Mater. Sci. Technol.*, 1997, vol. 13 (2), pp. 135–42.
25. A. Suzumura and Y.J. Xing: *Mater. Trans. JIM*, 1996, vol. 37 (5), pp. 1109–15.
26. J.R. Askew, J.F. Wilde, and T.I. Khan: *Mater. Sci. Technol.*, 1998, vol. 14 (9–10), pp. 920–24.
27. W.F. Gale and D.A. Butts: *Sci. Technol. Weld. Join.*, 2004, vol. 9 (4), pp. 283–300.
28. Y. Shen, W.F. Gale, J.W. Fergus, and X. Wen: *Mater. Sci. Technol.*, 2001, vol. 17 (10), pp. 1293–98.
29. Z.W. Xu, J.C. Yan, B.Y. Zhang, X.L. Kong, and S.Q. Yang: *Mater. Sci. Eng. A*, 2004, vol. 415, pp. 80–86.
30. Z.W. Xu, J.C. Yan, G.H. Wu, X.L. Kong, and S.Q. Yang: *Compos. Sci. Technol.*, 2005, vol. 65 (13), pp. 1959–63.

31. Z.W. Xu, J.C. Yan, C. Wang, and S.Q. Yang: *Mater. Chem. Phys.*, 2008, vol. 112 (3), pp. 831–37.
32. Y. Zhou, W.F. Gale, and T.H. North: *Int. Mater. Rev.*, 1995, vol. 40 (5), pp. 181–96.
33. G.O. Cook, III and C.D. Sorensen: *J. Mater. Sci.*, 2011, vol. 46, pp. 5305–23.
34. I. Tuah-poku, M. Dollar, and T.B. Massalski: *Metall Trans. A*, 1988, vol. 19, pp. 675–86.
35. W.H. Liu, D.Q. Sun, S.S. Jia, and X.M. Qiu: *Trans. China Weld. Inst.*, 2003, vol. 24 (5), pp. 13–16.
36. J. Yan, Z. Xu, G. Wu, and S. Yang: *Scripta Mater.*, 2004, vol. 51, pp. 147–50.
37. J. Maity and T.K. Pal: *J. Mater. Eng. Perform.*, 2012, vol. 21 (7), pp. 1232–42.
38. K.O. Cooke, T.I. Khan, and G.D. Oliver: *Metall. Mater. Trans. B*, 2013, vol. 44B, pp. 722–29.
39. J. Yan, Z. Xu, S. Lei, X. Ma, and S. Yang: *Mater. Des.*, 2011, vol. 32, pp. 343–47.
40. K.O. Cooke: *Metall. Mater. Trans. B*, 2012, vol. 43B, pp. 627–34.
41. W.P. Weng and T.H. Chuang: *Mater. Manuf. Process.*, 1997, vol. 12 (6), pp. 1107–32.
42. E. Lugscheider, S. Ferrara, H. Janssen, A. Reimann, and B. Wildpanner: *Microsyst. Technol.*, 2004, vol. 10 (3), pp. 233–36.
43. E. Lugscheider and S. Ferrara: *Adv. Eng. Mater.*, 2004, vol. 6 (3), pp. 160–63.
44. J. Huang, Y. Dong, Y. Wan, X. Zhao, and H. Zhang: *J. Mater. Process. Technol.*, 2007, vol. 190, pp. 312–16.
45. G.F. Zhang, J.X. Zhang, Y. Pei, S.Y. Li, and D.L. Chai: *Mater. Sci. Eng. A*, 2008, vol. 488, pp. 146–56.
46. G.F. Zhang, B. Chen, M.Z. Jin, and J.X. Zhang: *Mater. Trans.*, 2015, vol. 56 (2), pp. 212–17.
47. G.F. Zhang, X.J. Liao, B. Chen, L.J. Zhang, and J.X. Zhang: *Metall. Mater. Trans. A.*, 2015, vol. 46A, pp. 2568–78.
48. G.F. Zhang, W. Su, J.X. Zhang, and A. Suzumura: *J. Mater. Eng. Perform.*, 2013, vol. 22 (7), pp. 1982–94.
49. S. Ren, C. He, X. Qu, and Y. Li: *J. Alloys Compd.*, 2008, vol. 455, pp. 424–31.
50. J.C. Lee, J.P. Ahn, Z. Shi, J.H. Shim, and H.I. Lee: *Metall. Mater. Trans. A*, 2005, vol. 36A, pp. 3237–47.
51. W.M. Zhong, G. L'espérance, and M. Suéry: *Metall. Mater. Trans. A*, 1995, vol. 26A, pp. 2637–49.
52. G.F. Zhang, W. Su, J.X. Zhang, and A. Suzumura: *Trans Nonferrous Met. Soc. China*, 2012, vol. 22 (3), pp. 596 603.
53. K. Kotani, J.P. Jung, K. Ikeuchi, and F. Matsuda: *Trans. JWRI*, 1999, vol. 28 (2), pp. 27–37.
54. P. Shen, H. Fujii, T. Matsumoto, and K. Nogi: *Metall. Mater. Trans. A*, 2004, vol. 35A, pp. 583–88.
55. C.J. Hsu, C.Y. Chang, P.W. Kao, N.J. Ho, and C.P. Chang: *Acta Mater.*, 2006, vol. 54, pp. 5241–49.
56. M. Zeren and E. Karakulak: *J. Alloys Compd.*, 2008, vol. 450, pp. 255–59.
57. Y. Watanabe, N. Yamanaka, and Y. Fukui: *Metall. Mater. Trans. A*, 1999, vol. 30A, pp. 3253–61.